Mine Water and the Environment (2021) 40:189–208
https://doi.org/10.1007/s10230-020-00712-8

TECHNICAL ARTICLE

Interpretation of the Failure of the Aznalcóllar (Spain) Tailings Dam

Joaquín Martí[1,2] · **Francisco Riera**[2] · **Francisco Martínez**[2]

Received: 31 January 2020 / Accepted: 1 September 2020 / Published online: 18 September 2020

Abstract
The mechanisms and causes of the sudden failure of the Aznalcóllar tailings pond were investigated. The dam underwent displacements of up to 55 m along a 700 m length, releasing large quantities of acidic waters and 5.5 million m^3 of pyrite and pyroclastic tailings. It was a progressive type of failure, allowed by the brittle response of the pre-consolidated and cemented Guadalquivir blue clays and the high pore pressures left from the incomplete consolidation of the dam's foundation. Special modelling difficulties were posed by the need to incorporate the strain softening behaviour of the clays. The results show that although the timing of the failure could have been approximated using equivalent ductile properties, predicting the shallow, planar geometry of the failure surface observed would have required a precise representation of the brittle response. The failure triggered liquefaction of the tailings, which accelerated at more than 0.1 g. This transition was modelled by migrating from a coupled effective stress approach employing implicit integration to a total stress formulation using an explicit solver.

Keywords Progressive failure · Brittle behaviour · Numerical modelling

Introduction

On April 25, 1998 the dam bounding the tailings pond of the Aznalcóllar mine failed. As a consequence, there was an uncontrolled release of a substantial proportion of the stored materials, which contaminated rivers and large surfaces of land that required a series of mitigation and remediation measures. The mine was located near the town of Aznalcóllar, some 35 km northwest of Sevilla in southern Spain. It was one of a number of exploitations within the Andalusian pyrite belt. The accidental release of large quantities of acidic waters and mine tailings would have been of great concern under any circumstances but, in this case, was aggravated by the presence, downstream from the mine site, of a major bird sanctuary, the Doñana National Park. At the time of failure, the pond had operated uneventfully for about 20 years. Failure occurred suddenly, without any prior signs of distress, despite the instrumentation installed and its regular monitoring.

✉ Joaquín Martí
joaquin.marti@principia.es

[1] Madrid School of Mines, Ríos Rosas 21, 28003 Madrid, Spain

[2] Principia, Velázquez 94, 28006 Madrid, Spain

The accident has been studied by a number of teams. From a contamination and remediation viewpoint, an apt and early review was provided in a series of papers presented at the 1999 IMWA Congress in Sevilla, Spain (Fernández Rubio 1999). The designers of the pond, Intecsa and Geocisa, conducted their own post-failure geotechnical evaluation (Geocisa 2000). The regional government also commissioned a study, a summary of which has been published in the open literature (Olalla and Cuéllar 2001). The Courts, which eventually dismissed criminal proceedings against any of the parties, asked independent experts to analyse the case (Alonso and Gens 2000); their findings have been subsequently summarised in other publications (Alonso and Gens 2006a, b; Alonso et al. 2010; Gens and Alonso 2006). A more general description of the events, including some legal aspects, was presented by McDermott and Sibley (2000). Finally, the mining company, Boliden, also commissioned their own field and laboratory investigations (Botín and Ramírez Oyanguren 1999; EPTISA 1998), while the interpretation of the failure, the identification of its causes, and the necessary simulation work was entrusted to the authors.

The present paper takes all this information into account and concentrates on the numerical simulation and the interpretation of the failure. Previous investigators successfully determined the causes of the failure, but the role of brittleness and its influence in shaping the final failure surface

has remained uncertain. The investigations described here were conducted in the early 2000s, and peer-reviewed by an international committee (Norbert R. Morgenstern, Nilmar Janbu, Pedro Ramírez-Oyanguren, Jonny Sjöberg, and Howard Plewes), but the legal sensitivities of the case precluded their publication in the open technical literature at the time.

Description of the Facility

The original surface of the ground is almost horizontal, sloping very gently (on the order of a few percent) towards the east and southeast. The upper 4 m are constituted by granular deposits of alluvial origin and have a high permeability. The water table is usually located at the bottom of this layer, with occasional upward excursions in response to the infrequent precipitation events. The 70 m thick Guadalquivir blue clays appear directly underneath the surficial alluvium; their characteristics will be discussed in the next section. The sandstones and conglomerates underlying the clays are highly permeable and behave as a confined aquifer, known as the Niebla Posadas no. 26 aquifer, with slightly artesian pressures, with local pressures of 0.86 MPa (Alonso and Gens 2000; EPTISA 1998).

The tailings pond was approximately rectangular, covering an area of about 1 km by 2 km. It was divided into two compartments because the original design contemplated separate storage of pyroclastic and pyrite tailings, although only the latter were discharged in both ponds since the late 1980s (Fig. 1). The failure occurred along the east wall of the southern pond, which contained only pyritic tailings. The river Agrio, usually with little or no water, runs immediately to the east of the pond.

The facility was initially designed by Intecsa (1978) and construction started swiftly thereafter. The stability of the as-built dam was later reassessed by Geocisa (1996a), who also introduced some small design modifications (Geocisa 1996b); the main one was an increase of 1.5 m in the final design elevation for the crest of the southern dam, thus reaching the same elevation foreseen for the northern one.

The main body of the dam was built with unclassified waste rock from the mining operations. It is a schist rock and

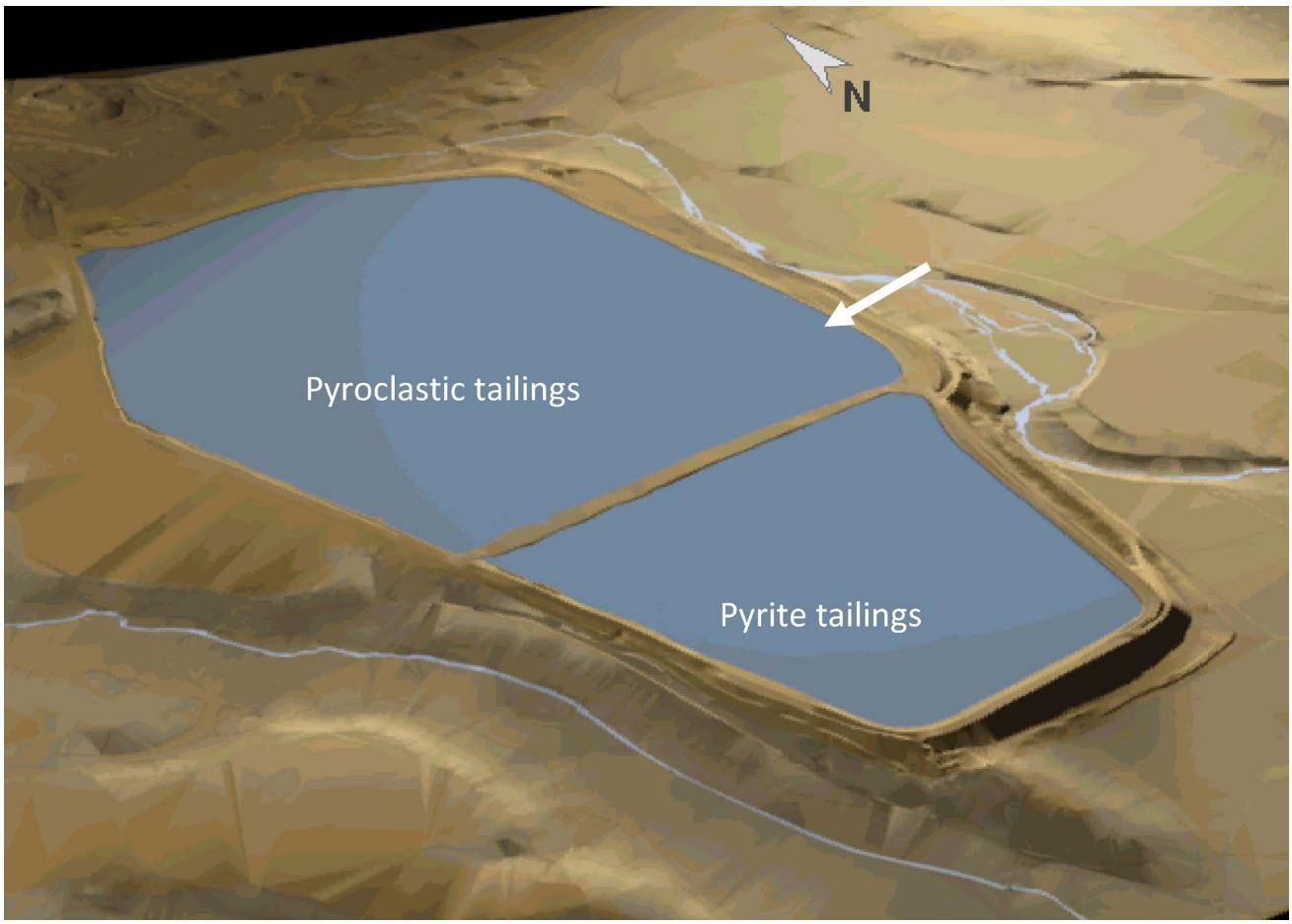

Fig. 1 View of a model of the Aznalcóllar tailings pond

contained a wide range of sizes, from metric size boulders to fines; the latter represent about 30%. As placed in the dam, the material had a bulk density of 2100 kg/m^3 and angle of effective friction of 40°.

To ensure adequate containment, a low-permeability clayey material, the red *rañas,* was placed on the upstream face of the dam, with a graded sand acting as a filter. In the dam, the *rañas* had a density of 2170 kg/m^3, an angle of effective friction of 27°, and a hydraulic conductivity of 10^{-9} m/s. The initial project called for horizontal thicknesses of 4 m for the *rañas* and 3 m for the filter. The enlargement project maintained the global thickness of 7 m, but suppressed the filter at the higher elevations, where pressure gradients would always remain small. To prevent seepage through the alluvial deposits, a cement bentonite barrier extended downwards from the low permeability *rañas* 1 m into the blue clays.

The initial slopes were 1(V):1.9(H) (27.8°) for the upstream face of the dam and 1(V):1.75(H) (29.7°) for the downstream face, with a width at the top of 14 m. In the modified project, the downstream face was steepened to 1(V): 1.3(H) (37.6°), while the width at the crest was enlarged in areas close to the river. In practical terms, the modified design differed relatively little from the original one, since the increased width tended to compensate for the steeper slope. The more notable difference is that a steeper downstream slope enhances the stress concentration under the toe.

Construction of the dam proceeded over some 20 years, at the pace demanded by tailings disposal needs. A freeboard of 1 m was kept above the level of the ponded water and tailings. The evolution of dam heights and its idealisation for analysis can be seen in Fig. 2; Fig. 3 shows the corresponding cross-sections. The final design height was 30 m, of which 27 m were built when failure occurred.

The tailings of interest were pyritic, since they were the only ones ponded at the failure location; they were a non-cohesive material, made of relatively fine particles on the order of tens of microns. The density of the solids was 4800 kg/m^3 and the bulk density was 2950 kg/m^3. They were

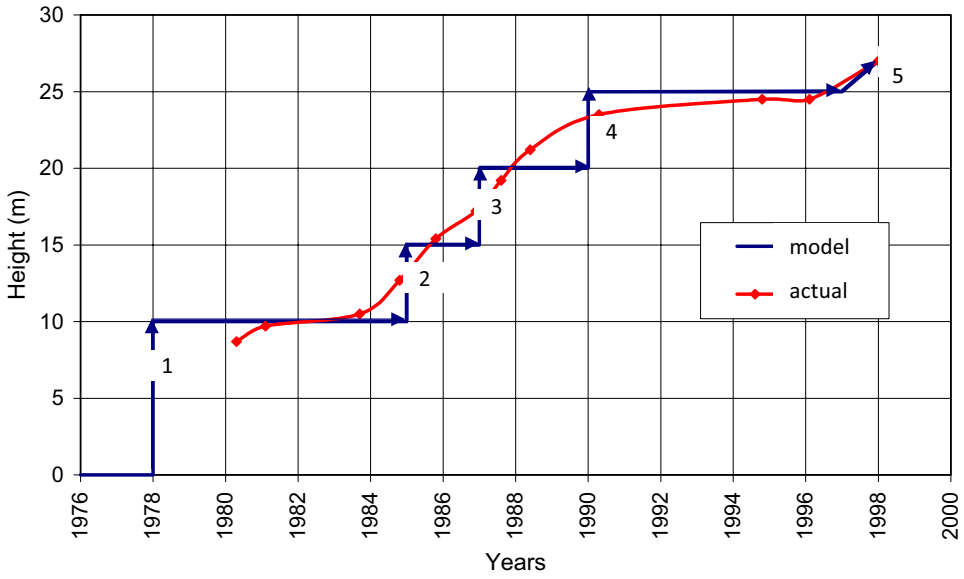

Fig. 2 Actual and idealised evolution of dam heights

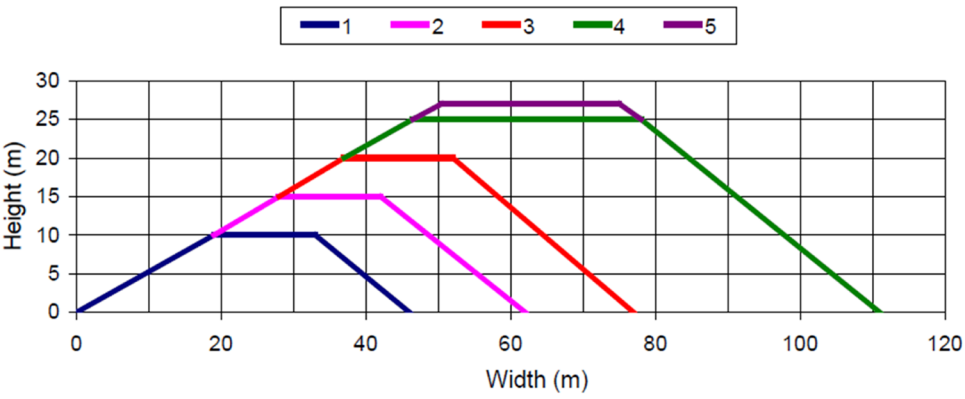

Fig. 3 Evolution of heights and cross-sections of the dam

transported in water and discharged into the pond; the solid particles settled and the water, which had covered the solids, was recycled. Because of their mode of deposition, the tailings initially adopted a relatively loose structure, which tended to densify when disturbed. However, it appears that over time they acquired some cementation and, in fact, the precise mechanism that triggered their liquefaction remains somewhat elusive; static tests conducted for this purpose at the School of Civil Engineering in Barcelona were unable to replicate it.

Guadalquivir Blue Clays

The Guadalquivir blue clays underlying the alluvial terrace were heavily over-consolidated, fissured, carbonate-rich clays of high plasticity, dating from the Lower Messinian (Upper Miocene). Their bulk density was 1900 kg/m^3 with a density of solids of 2690 kg/m^3. The liquid and plastic limits averaged about 64 and 27%, respectively.

The blue clays display brittle behaviour, a concept introduced by Skempton (1964): once remoulded or sheared past their peak strength, their residual strength is much lower. The brittle character of these clays was known in the 1970s (Fernández Blanco 1979) and knowledge improved over the years because their pervasive presence gave rise to recurrent problems (Sevilla metro, highway and railway slope failures, etc.); Oteo and Sola (1993) present a more precise account of this brittleness.

Various determinations of the peak strength of the blue clays at Aznalcóllar are available (see Table 1). Those by Intecsa and Geocisa were made before the failure and do not recognise the brittle character of the strength. Of the other two, the more thorough one is probably that by Alonso and Gens (2000). Their higher peak values probably was due because they tended to rely on direct shear tests, a test that strongly constrains the location of the failure; indeed, other tests (simple shear and triaxial) generated lower peak strengths with less abrupt brittleness.

Figure 4 shows a typical curve depicting shear stress vs relative displacement, produced in ring shear tests conducted on undisturbed samples by the Norwegian Geotechnical Institute at Eptisa's request; similar behaviour was observed

Table 1 Peak strength of the blue clays

	Peak cohesion c'_p (kPa)	Peak friction φ'_p (degrees)
Intecsa (1978)	0	25
Geocisa (1996a, b)	20	22
Eptisa (1998)	26	20
Alonso and Gens (2000)	65	24

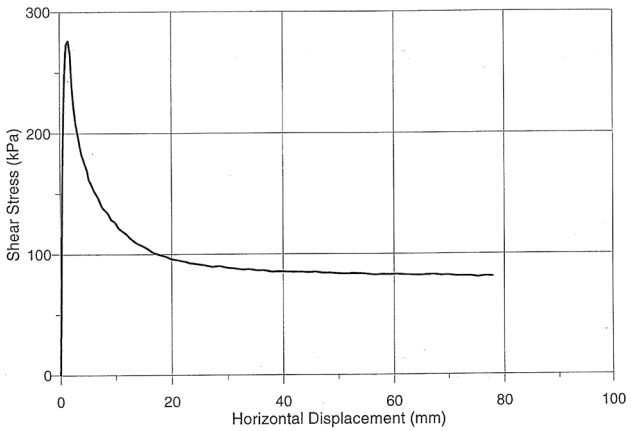

Fig. 4 Brittle behaviour evinced in ring shear tests

by Alonso and Gens (2000). In direct shear tests, cohesion vanished over displacements on the order of 1 mm, while friction evolved to its residual value over relative displacements an order of magnitude greater. There was wide consensus that the residual strength was characterised by 12° friction and null cohesion. Figure 5 presents the idealised stress–strain curve, with cohesion and friction decreasing to their residual values over different strains. This type of behaviour has also been subsequently observed in the context of the neighbouring Las Cruces mining operations (Cooper et al 2019; Galera et al. 2009).

The local structure of the clays includes subhorizontal sets of bedding planes, as well as two subvertical sets of closed fissures, one trending N–S and the other NE–SW.

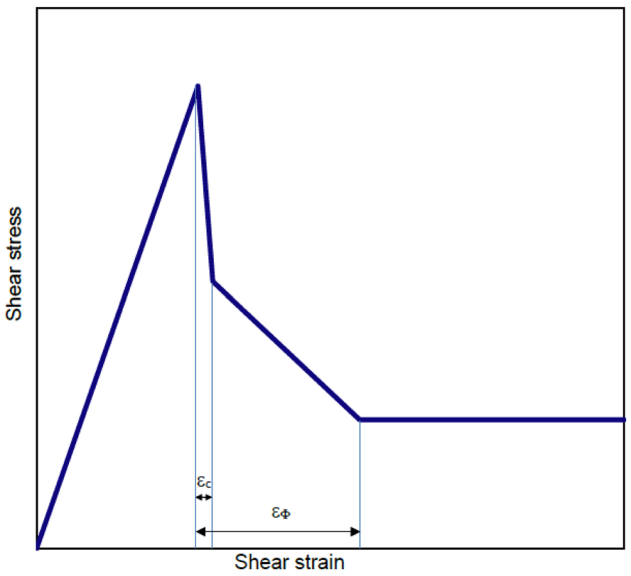

Fig. 5 Brittle behaviour modelled, showing the loss of cohesion and reduction of friction

The clays themselves are fairly homogeneous and display relatively little anisotropy. The strength does not seem to be much less along bedding planes: indeed, Alonso and Gens (2000) conducted tests at different orientations and the effects were no greater than the data's natural scatter.

An important characteristic of the blue clays is their very low permeability which, together with their 70 m thickness, leads to very long consolidation times. Their coefficient of consolidation is 0.001 cm^2/s. This determination is consistent both with the results of consolidation tests in the laboratory and with the pore pressures recorded in the field by the piezometers installed after the failure. Such consistency is expected in a massive formation, devoid of preferential paths for water migration.

The pre-existing stress state in the clays is not known with certainty. Measurements taken in adjacent formations at nearby locations suggest that the ratio of horizontal to vertical stresses (K_0) was about 1 or marginally lower.

Description of the Failure

The dam failed during the morning of April 25, 1998, causing a large spill into the nearby the River Agrio; the spilled volumes of tailings and water are estimated at 1.3 and 5.5 million m^3, respectively. Failure probably occurred shortly before 01:00, when the power line near the dam toe failed. The maximum outflow took place sometime between 01:00 and 03:00, as evidenced by the peak water level recorded at 03:30 by the staff-gage located 13 km downstream. The outflow discharge ceased around 08:00, when the river flow at the staff-gage started to decline, returning to normal by 18:00. Figure 6 presents a photograph of the breach.

During the failure, the dam experienced up to 55 m of lateral displacement, with few distortions, along a 700 m long segment of the east dam of the pyrite pond (Fig. 7). The dam, together with the alluvium layer and the upper 10 m of clays below the alluvium, formed a block that slid along a near-horizontal surface in a direction approximately perpendicular to the dam. Figure 8 shows the cross-section of the dam before and after the failure. These two figures are adapted from Alonso and Gens 2006a).

Fig. 6 Breach produced by the failure

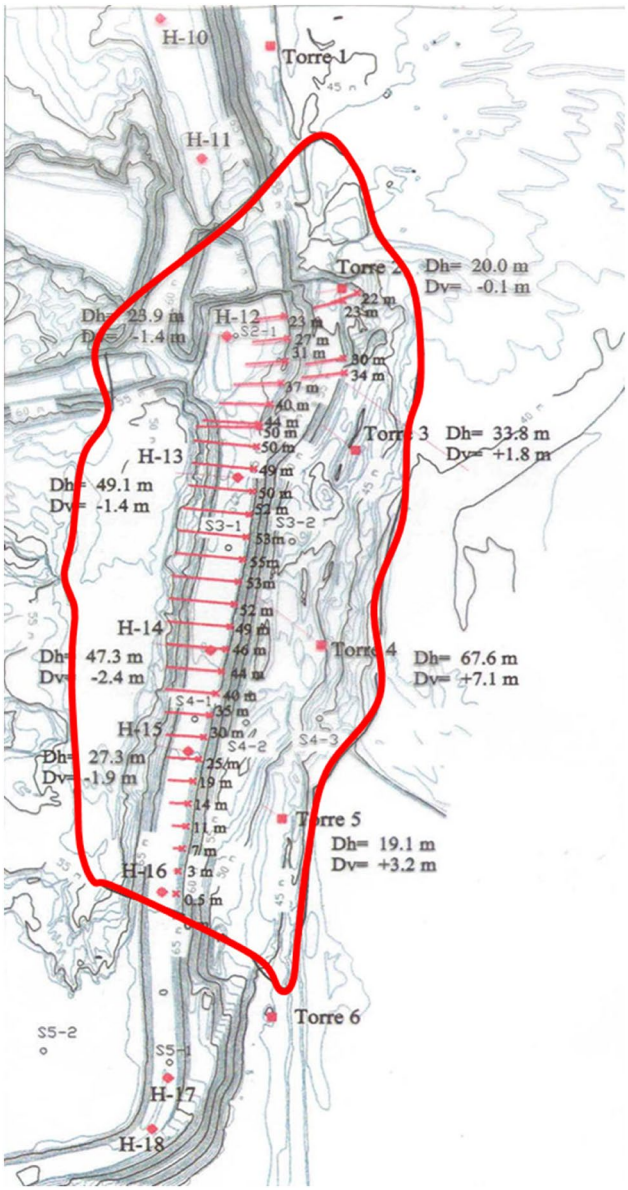

Fig. 7 Plan view of the failure indicating dam displacements (adapted from Alonso and Gens 2006a)

At the northern end of the failure zone, near the southeast comer of the pyroclastic tailings pond, the southern part of the dam separated from the northern part. The spill breach was initially formed in this area and then enlarged by erosion. The lateral displacements were largest at the centre of the failure zone and decreased gradually towards the south.

The upstream end of the displaced block was a near-vertical surface located beneath the area occupied by the tailings. The downstream exit of the slide was an oblique shear cut of the clays, producing upward folding, bulging, and over-thrusting.

After the failure, the tailings within the pyrite pond showed a large flat surface with numerous liquefaction craters; widespread tailings liquefaction occurred in a large zone within the pyrite pond, where tailings flowed out of the pond in the initial stages of the breach. On the other hand, pyroclastic tailings, coarser than the pyritic tailings, did not liquefy and their release was mainly due to water erosion.

The early liquefaction of the pyritic tailings involved only a relatively small volume of materials. There is some direct evidence of this (a near-vertical slope left in the tailings), as well as indirect evidence (the gradual decrease of the force pushing the dam, which kept displacements from being even greater).

The degree with which the dam maintained its integrity, while undergoing a displacement of 55 m, is remarkable and indicates that, above the ground surface, the dam was safely designed and built. The large displacements were possible because: a) strain softening leads to diminishing strengths along the failure surface once sliding starts, and b) tailings liquefaction increases the horizontal forces on the dam and allows maintaining them during its movement. The latter occurred because the loss of shear strength of the tailings made them behave essentially as a liquid; rather than exerting simply an at-rest pressure, they applied the hydrostatic pressure associated with their bulk density to the dam.

It is interesting to note that the failure surface did not remain exactly the same for the complete failure process. Conditions prevailing until the onset of failure may have led

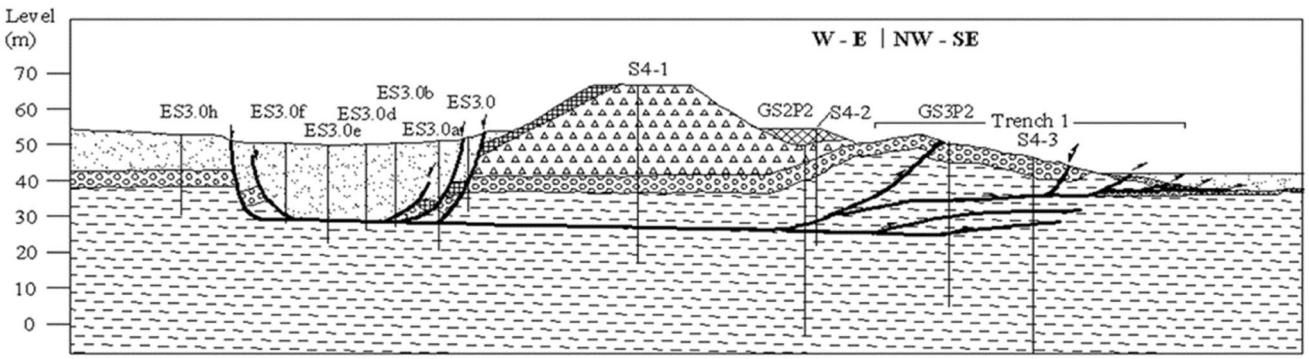

Fig. 8 Final geometry of the observed failure and initial position (adapted from Alonso and Gens 2006a)

to failure along a given surface, but as failure started, liquefaction of the tailings drastically changed the configuration of loading, and failure could then proceed along a somewhat different surface from that initially activated.

Monitoring Information

Some instrumentation had been placed and monitored by Geocisa (1998), providing data over the last 15 months before the accident. The monitoring activities included visual inspections, as well as periodic measurements taken from four inclinometers, 22 settlement plates and four piezometers. Several factors, though, limit the usefulness of the data.

No piezometers penetrated into the blue clays. Hence, they simply recorded the fluctuations of the phreatic surface within the alluvial deposit, suspended above the low-permeability clays, in response to the variable regime of precipitations. They would have been useful for detecting leakage problems, which was the main reason for installing them, but they could not yield information about the progress of consolidation.

Of greater interest was inclinometer I-3, since it was located in the area that suffered the largest displacements. Figure 9 shows its traces during the monitoring period, starting in December 1996. Unfortunately, inclinometer

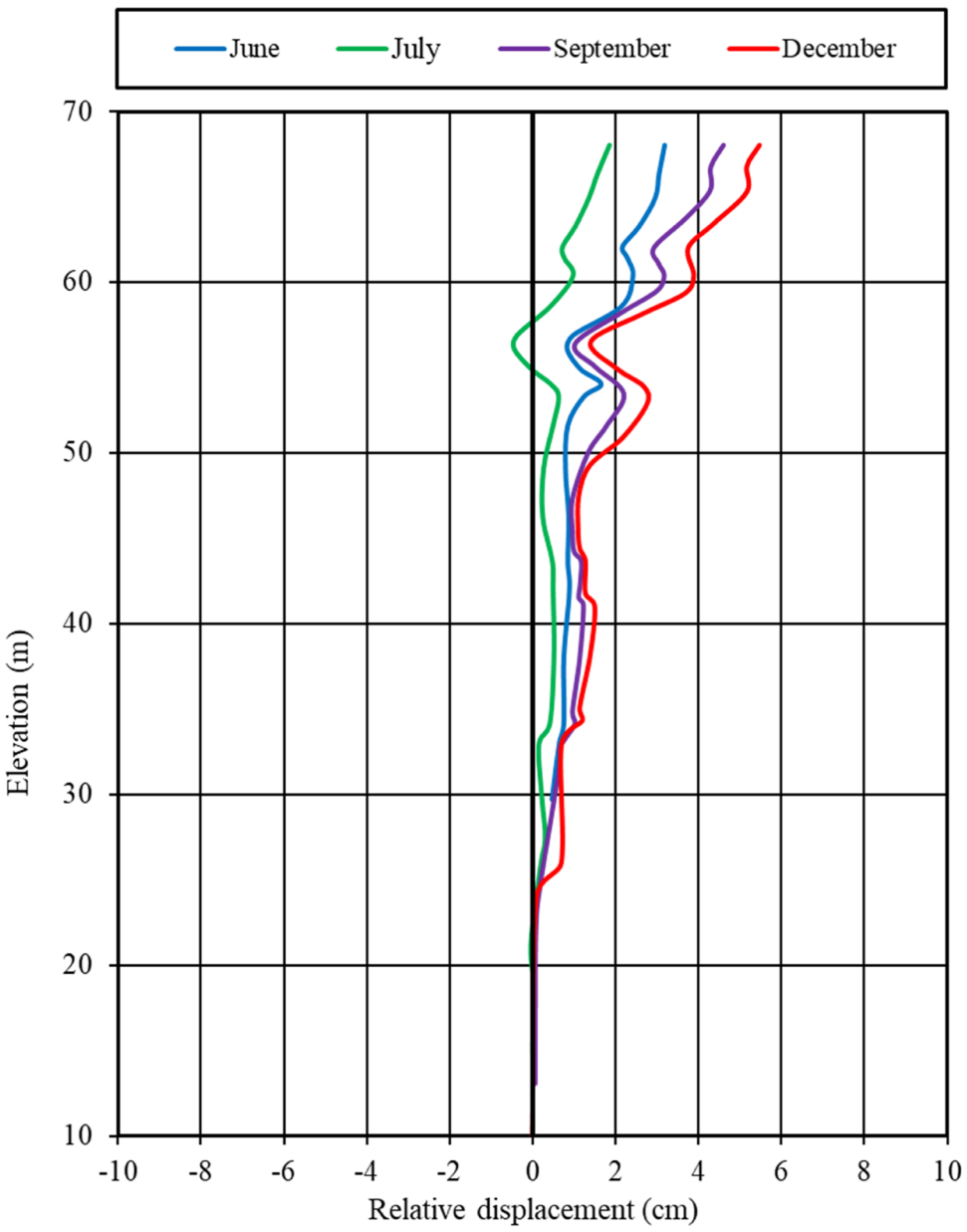

Fig. 9 Traces from inclinometer I-3

I-3 was damaged at a depth of about 5 m shortly after January 1998 and provided no data thereafter. At the end of 1997, I-3 was experiencing a uniform displacement of 1 cm from elevation 25–50 masl; above 50 m, the displacement grew, with some oscillations, to reach about 5 cm at the top of the dam (i.e. at an elevation of 68 m).

The shallower feature of the inclinometer trace consisted of gradually increasing displacements, starting at about elevation 50 m. This point is about 8 m inside the body of the dam, which suffered no disruptions, even in the course of the large failure displacement. The most likely origin was a local disturbance, produced by the ongoing construction, perhaps involving rearrangement of schist blocks and buckling of the inclinometer tube.

The deeper feature was a displacement of about 1 cm at an elevation of 25 m, about 3–4 m deeper than the plane where the sliding occurred. This discontinuity, although small, is more suggestive of a failure mechanism being activated within the clay. Interpreting this feature presents some problems, though, as any calculations must be based on the local increase of the levels of the tailings and water. Over this period, the level of water increased 0.95 m, from 65.50 m to 66.45 m. It seems that no tailings were placed in the failure area over this period; hence, for quantitative comparisons, it will be assumed that the displacements recorded were caused by a 0.95 m increase in the water elevation in the pond; while the increase in water level was taking place, tailings elevations were between 24 and 26 m. Although potentially useful in the context of a forensic investigation, the impending character of the failure would have been difficult to infer at the time from the readings of inclinometer I-3.

Modelling Approach

Since the events experienced by the dam varied only slightly with location along its north–south axis, particularly around the region of maximum displacement, the problem can be analysed in plane strain. All materials above the bottom of the clays were represented in the computer model. To provide good boundary conditions below the clays, some of the underlying strata were also modelled. Horizontally, the model was extended sufficiently far from the dam to avoid interference with the solution of the problem. The mesh generated is presented in Fig. 10. The various materials are colour coded in the figure. The elements were organised to allow a phased construction.

Construction was simulated in five phases using the cross-sections in Fig. 3. However, for phases 2 to 5, the gravity loads of the added materials were introduced gradually, spanning a period of two years for each, except for phase 4 where the loading lasted three years, and was followed by five years of inactivity.

Mechanical Behaviour and Conditions

Essentially all materials were considered elastoplastic using a Mohr–Coulomb criterion. In the case of the clays, straining past the peak gradually decreases the strength towards a residual value. Tailings liquefaction also implies weakening through deformation, but this event was not considered to precede the failure.

In most cases, all the natural materials were assumed to start from an isotropic state of effective stresses; then, as the dam and the tailings rose, the stresses at each point were free to evolve in response. A small number of cases were analysed with non-isotropic initial stresses.

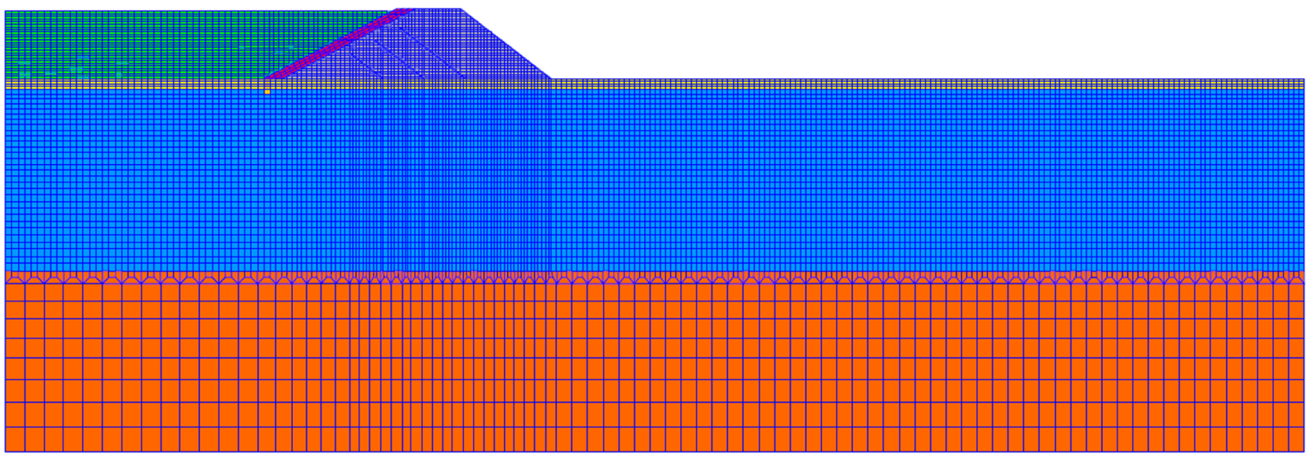

Fig. 10 Global mesh used in the calculations

The upper surface of the model was kept free of any loads. The two vertical side boundaries of the model only constrained movements in the horizontal direction. At the bottom of the model, all movement was considered to be negligible. The only mechanical loading imposed was the weight of the various materials.

Hydraulic Behaviour and Model Conditions

Water flow was assumed to follow Darcy's law. No hydraulic calculations were carried out in the materials that seemed to be of little relevance: the underlying sandstones, the alluvium downstream from the cement bentonite wall, the dam body, and the core and filter material. The upstream face of the dam and the cement bentonite barrier were taken as impermeable, an adequate hypothesis from the viewpoint of the forces on the dam.

The initial water table was located at the clay-alluvium interface. At the bottom of the clays, the water pressure was set at 0.86 MPa, corresponding to the local pressures in the Niebla Posadas aquifer. Initially, a steady-state, linear distribution of water pressures was assumed to exist between these two depths, and the water pressures in the aquifer were assumed to be unaffected by construction. Likewise, downstream from the cement bentonite barrier, the water table was kept at the clay-alluvium interface.

Within the pond, though, pore pressures evolved freely with the water table at the outer surface. The consolidation of the tailings was independently studied using the solution given by Gibson (1958); the maximum excess pore pressures generated within the tailings were only on the order of 1–3% of the effective pressures, depending on whether the alluvium was assumed to drain or not.

No flow was allowed across the vertical side boundaries of the model for either the tailings or the clays. However, the alluvium was considered sufficiently permeable for its pressures to remain hydrostatic; thus, at the upstream vertical boundary of the alluvium, the pressures were kept in hydrostatic balance with the position of the water table above.

Numerical Procedures

Given their thickness and consolidation characteristics, only a very small percentage of the construction-induced pore pressures can dissipate during the 20-year construction. Thus, a coupled analysis was performed, simultaneously tracking the evolution of the structural and pore water processes. The program used was ABAQUS/Standard (HKS 1998a), employing implicit time integration, which is ideal in a slow marching problem and allows the solution to progress in large time increments. Once failure starts and the tailings liquefy, this procedure is no longer appropriate because of the accelerations induced by the new forces generated; explicit integration is now more appropriate and, since the process is fast, there is no further need for a coupled solution. The program used for this new task was ABAQUS/Explicit (HKS 1998b).

The migration procedure is complicated because it involves the transfer of a coupled solution (soil and water independently treated), obtained using one type of elements, to a non-coupled approach (total stress treatment), based on a different set of elements. The migration must preserve the idiosyncrasies of the ongoing failure: weakened regions, effective stresses, etc. Some of these complications would have been easier to handle with current versions of the software (SIMULIA 2019), which allow using the same material descriptions in the pre-failure (implicit) and the post-failure (explicit) calculations, including the softening undergone by the cohesive and frictional components of the strength.

In any case, the strain softening of the clays poses severe difficulties, as there are still no well-established procedures for modelling this behaviour in a way that is fully objective with respect to mesh and element type models. There are only two ways to this:

(a) To deprive the model of this distinctive aspect of the clays' behaviour, which played a major role in the failure. Brittleness then cannot be accounted for except qualitatively or by using "equivalent" ductile properties.
(b) To introduce strain softening in the model, knowing that the material parameters would need to be altered if the mesh changed; this does not necessarily invalidate the results, but it does require special care in their interpretation. This was the option adopted here.

A mesh size of 2 m was used for an affordable computational effort at the time. Since the constitutive model describes stress as a function of strain (not displacement), the characteristic element size affects the consistent parameters of the material. With fully integrated elements and 2×2 Gauss points covering half the element length, a relative displacement of 1 mm translates to a strain on the order of 0.001.

It must be pointed out that, subsequently to the work reported here, the problem was revisited using the material point method (MPM) for introducing the detailed brittle behaviour (Alonso and Zabala 2012; Zabala and Alonso 2011). The results are fairly consistent with those presented here and the MPM provides a valuable alternative for dealing with this type of problems.

Simulation of Pre-Liquefaction Events

Using the procedures described, the construction was followed step by step. The analyses must account for natural variability in the materials, as well as for the uncertainty

associated with any experimental determination of their properties. Furthermore, a forensic investigation must also be able to answer "what if" questions. For these reasons, the key parameters were assigned ranges of variation:

(a) coefficient of consolidation: $C_v = 0.001–0.002$ cm^2/s
(b) effective cohesion: $c'_p = 0$ to 65 kPa for the peak value, decreasing to 0 kPa over strains between 0.001 and 0.1
(c) effective friction angle: $\varphi' = 24°$ for the peak value, decreasing to 12° over strains between 0.02 and 0.1

In addition, the influence of other less important parameters was also investigated:

- stiffness of the dam body
- mechanical and consolidation characteristics of the tailings
- dilatancy of the alluvium
- deformation levels in the blue clays at which the peak strength develops
- pre-existing ratio of horizontal to vertical stresses within the blue clays

About one hundred calculations were carried out using various combinations of parameters.

Results with 65 kPa Peak Cohesion

The progressive application of the construction loads increases the pore pressures in the clays; these pressures, gradually but very slowly, dissipate, with a corresponding increase in effective stresses. There is no delay though for the shear stresses; they are activated as soon as the growing dam and pond generate the loads.

Figure 11 shows a typical result, using in this case a peak cohesion of 65 kPa. It depicts the levels of plastic strains immediately before failure, which occurred when the dam was 25 m high. The coefficient of consolidation was 0.001 cm^2/s, residual friction was reached for 0.02 strains, and residual cohesion for 0.001 strains. As the figure shows, the strain levels are such that the strength has already decreased to its residual value at all points of the failure surface.

From the upstream toe, the failure is very well developed and curves rapidly to become more horizontal within the clays. Around the downstream toe, the failure surface is a typical deep surface under the toe which, rather than continuing its curvature upwards through the dam, finds it easier to link up with the incipient failure surface going through

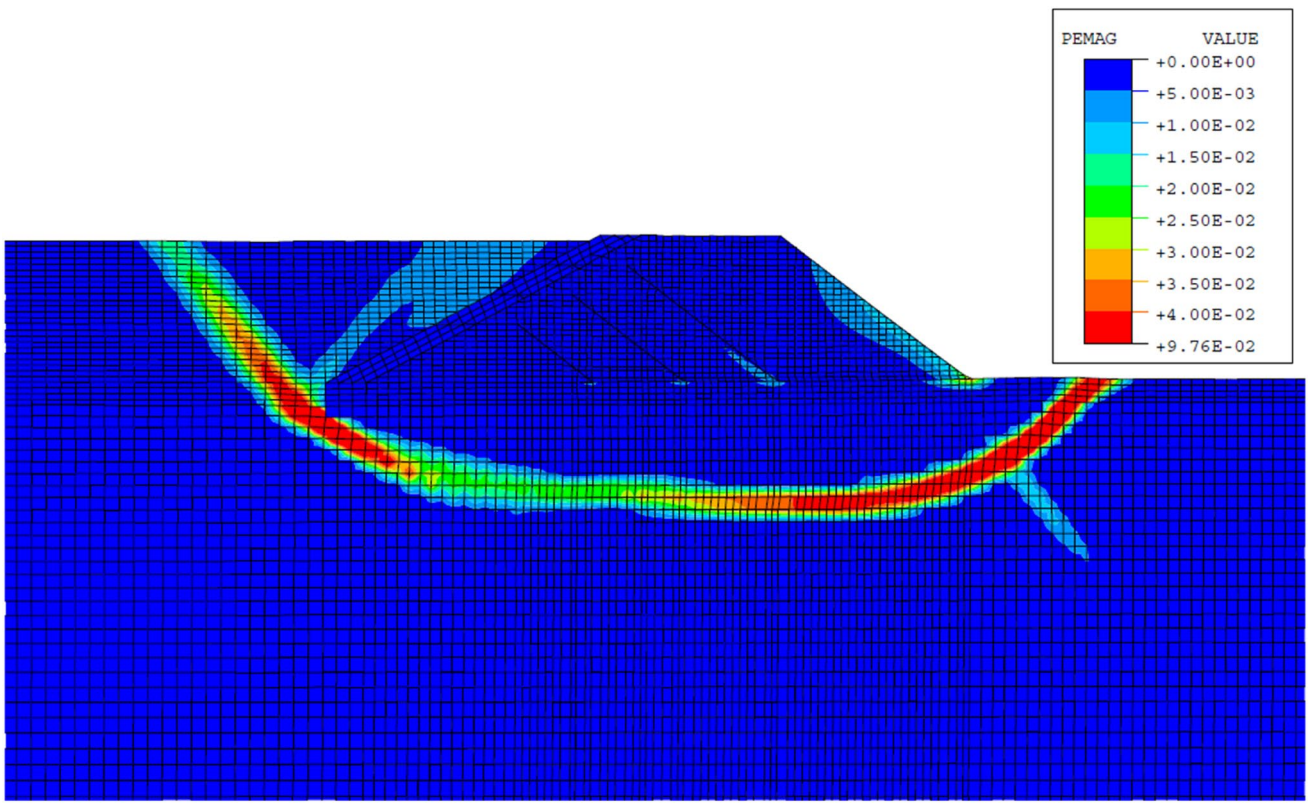

Fig. 11 Plastic strains at about 25 m ($C_v = 0.001$ cm^2/s; $\varepsilon_c = 0.001$; $\varepsilon_\varphi = 0.02$)

the upstream toe. The central part of the failure is the last one to develop. The linkage of the two, initially independent, failure surfaces results in a rather planar surface, which in this case extends about 16 m below the top of the clays.

Minor variations in the above parameters maintain the timing and approximate geometry of the failure. However, if the material is sufficiently ductile, failure does not occur, even when the dam reaches 27 m in April 1998. Figure 12 shows the plastic strains at that time when cohesion vanishes only for 0.005 strains and the residual friction is attained after reaching 0.1 strains. The failure surface is already developing and only the central upstream region remains intact. The dam is very close to failure and only the residual strengths can be mobilised over a large region of an eventual failure surface. Also, the progressive failure is clear in this figure: a small additional increment in dam height (and in the associated forces exerted by the tailings) will complete the progressively extending failure surface. When this happens, the failure will be essentially planar and will traverse the clays some 12–14 m below the contact with the alluvium.

If a marked brittleness is maintained (0.001 strains for the cohesion and 0.02 for the residual friction), avoiding the failure at elevation 27 m requires increasing the coefficient of consolidation to about 0.00175 cm^2/s. At a value of 0.00150 cm^2/s, failure still occurs before reaching the height of 27 m (Fig. 13).

As a final observation, the dam was very near failure in 1987, when it reached a height of 20 m. An analysis was carried out using the values employed by Geocisa (1996a, 1996b), that is, $\varphi' = 22°$ and $c'_p = 20$ kPa, for the peak strength of the clays. The rest of the parameters were identical to those used for producing Fig. 11. The calculations predict failure in 1987, shortly before reaching the height of 20 m (Fig. 14).

Balance between Peak Cohesion and Brittleness

The previous section investigated the expected outcomes for a peak cohesion of 65 kPa, as reported by Alonso and Gens (2000). However, this value is known to diminish and to be somewhat less brittle when determined by tests other than direct shear; thus, an effort was made to determine the combinations of peak cohesion c'_p and degree of brittleness that would be consistent with the timing of the failure. The degree of brittleness was quantified here by the level of plastic strain ε_c over which the initial cohesion (peak cohesion) went to zero (residual cohesion).

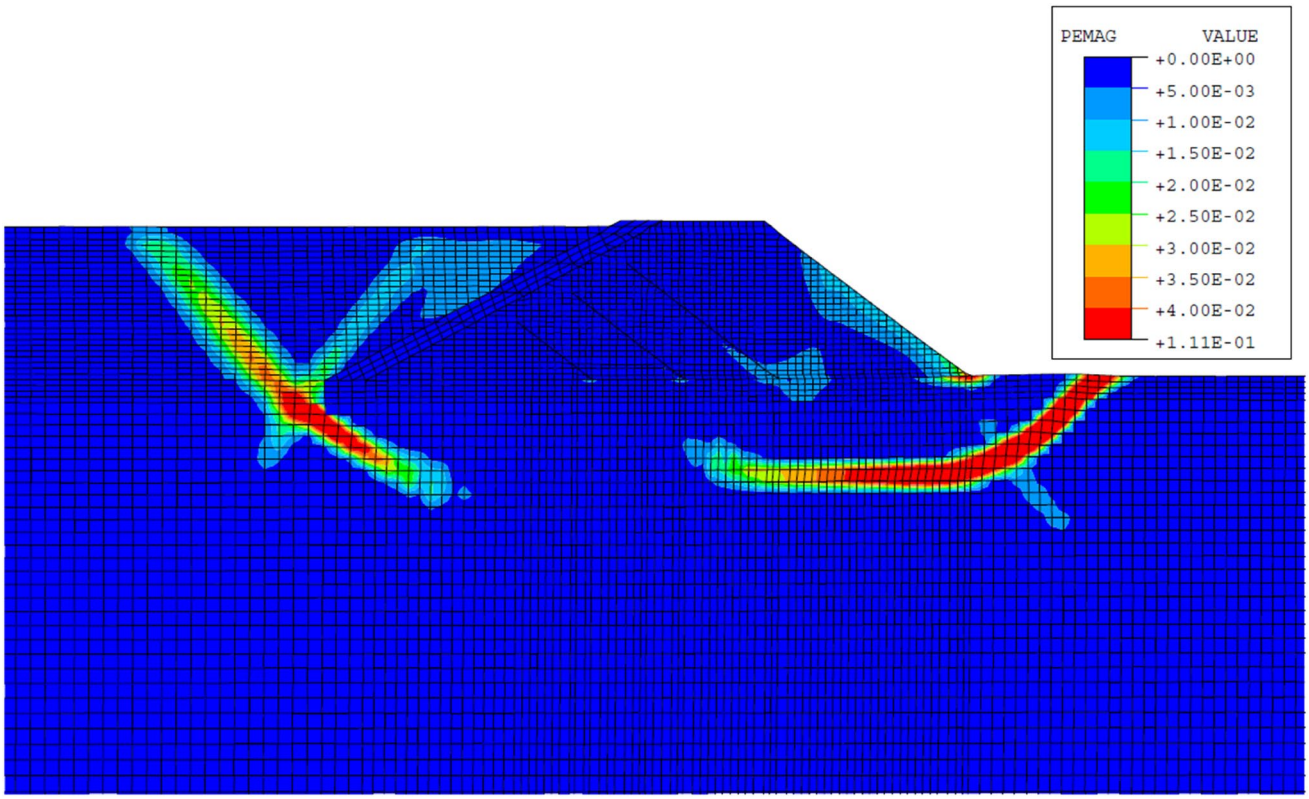

Fig. 12 Plastic strains at about 27 m ($C_v = 0.001$ cm^2/s; $\varepsilon_c = 0.005$; $\varepsilon_\varphi = 0.10$)

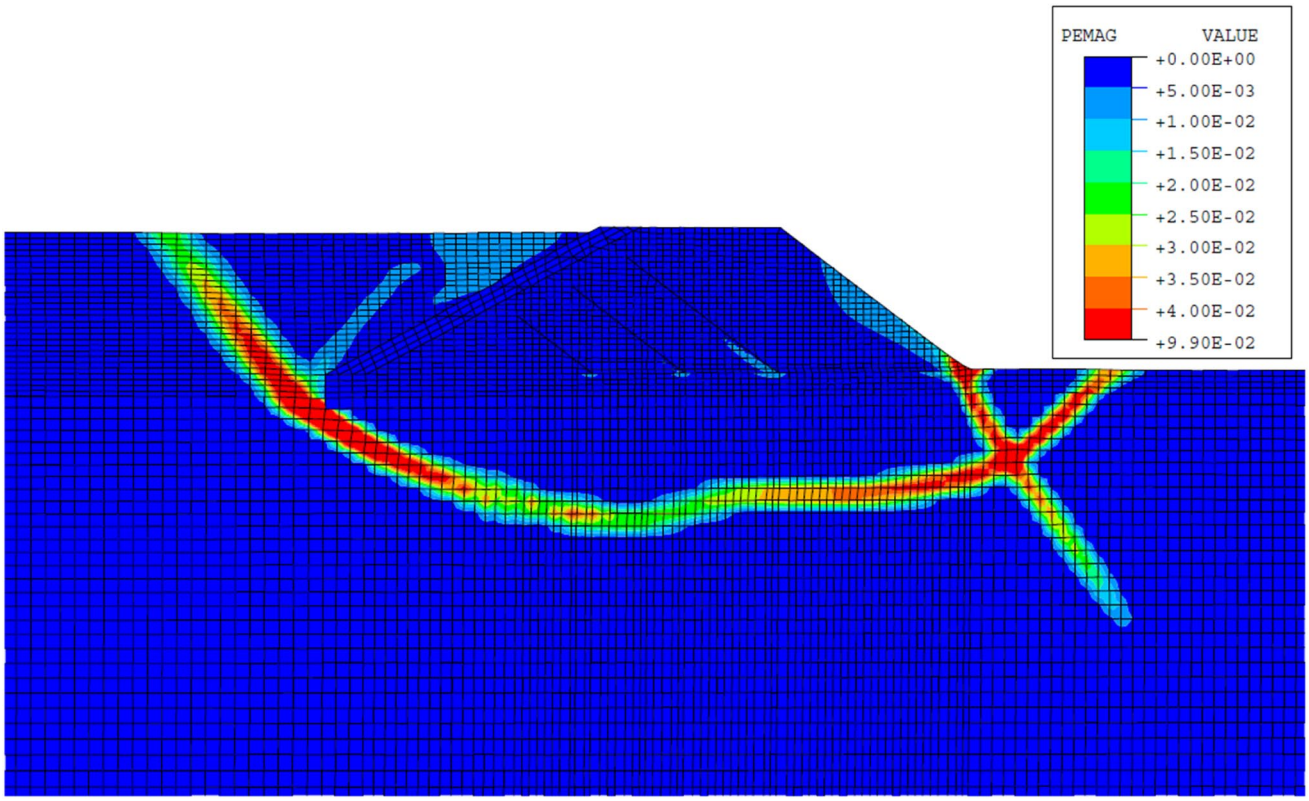

Fig. 13 Plastic strains at about 25 m ($C_v = 0.0015$ cm^2/s; $\varepsilon_c = 0.001$; $\varepsilon_\varphi = 0.02$)

The investigation was carried out by repeating the calculations for selected combinations of c'_p and ε_c and observing whether failure was predicted before or after April 1998 (a height of 27 m). The results are summarised in Fig. 15, where the conditions leading to an early failure are represented with red circles, while those allowing survival past April 1998 are indicated by blue circles. The dashed line approximately separates the two regions. The effects of brittleness are quite important, at least while ε_c is below about 0.02. In that range, moderate changes in ε_c require drastic variations in the peak cohesion c'_p needed to match the timing of the failure; after 0.02, further increases in ductility have a much smaller impact on the peak cohesion required. In principle, any combination of c'_p and ε_c located along the dashed line will result in failure in April 1998.

Apart from the timing, other things are also known about the failure: in particular, the failure surface that developed was planar and shallow, located some 10–12 m within the clays. As seen earlier, a marked brittleness naturally results in failure surfaces that are roughly consistent with the observed characteristics. However, this is not the case when failure occurs with greater ductility and less peak cohesion. There is no need to provide here the failure configurations resulting in each of the cases shown in Fig. 13, but Fig. 16 gives an insight; it corresponds to a case with $c'_p = 20$ kPa and $\varepsilon_c = 0.06$, which fails immediately before April 1998. As the figure shows, the surface is no longer a shallow plane, but deeper and more smoothly curved.

This observation is shared by all failure surfaces resulting from assuming less brittleness. To quantify this, each degree of brittleness, characterised by ε_c, has been plotted against the depth of the failure surface (Fig. 17) that results when the peak cohesion is chosen to produce failure in April 1998. The error bands shown in the figure span one element dimension in each direction.

As seen in the figure, all the more ductile hypotheses (ε_c greater than about 0.015 or 0.02) led to deeper failure surfaces, descending some 25 m inside the clays. However, as the clays become more brittle, progressively shallower and more planar failure surfaces are predicted. Figure 15 would allow expressing this effect in terms of peak cohesion. Clearly, failure surface depths on the order of 10–12 m require a very brittle behaviour (ε_c below 0.004) and a peak cohesion at or near the value of 65 kPa reported by Alonso and Gens.

The foregoing does not necessarily imply that consistency with the observed failure surface requires $c'_p = 65$ kPa and $\varepsilon_c = 0.003$. If the clays were actually weaker when deformed

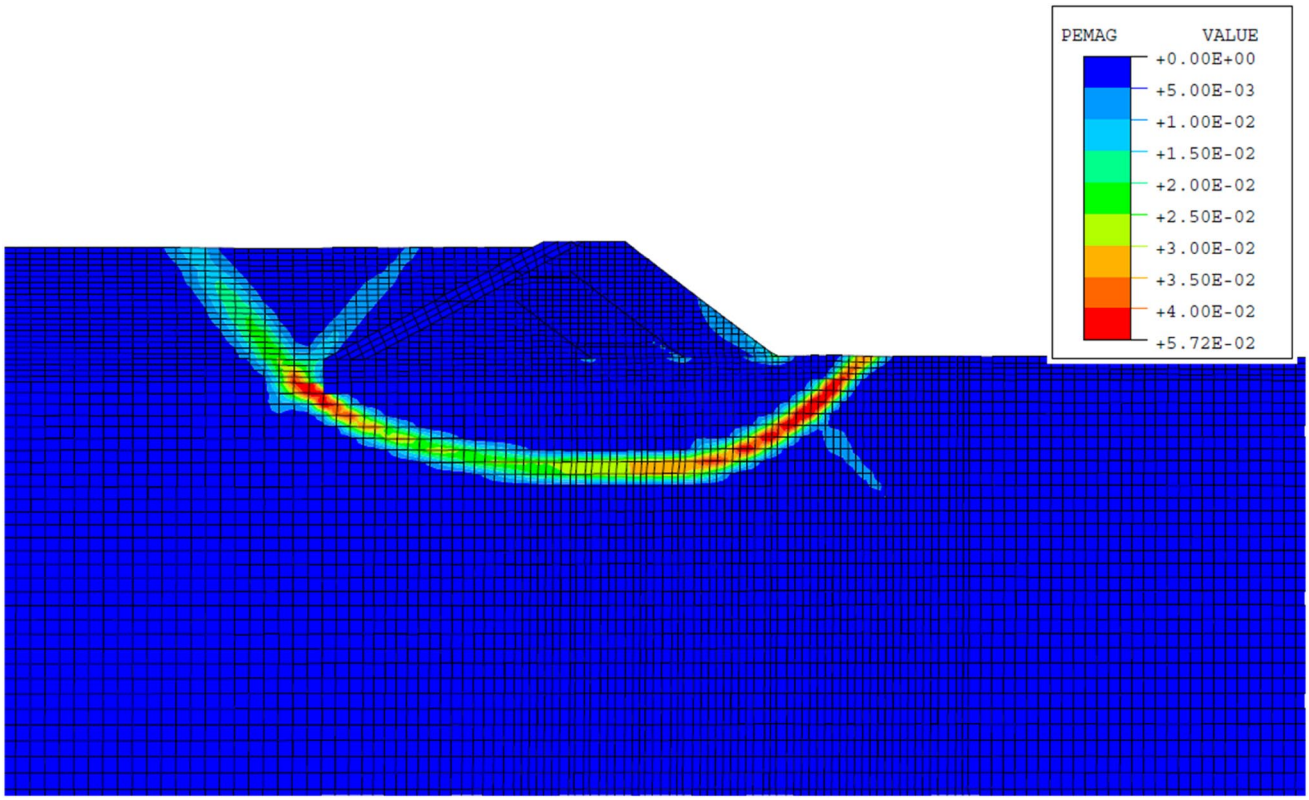

Fig. 14 Plastic strains at failure in 1987. Peak strengths from Geocisa (1996a, b)

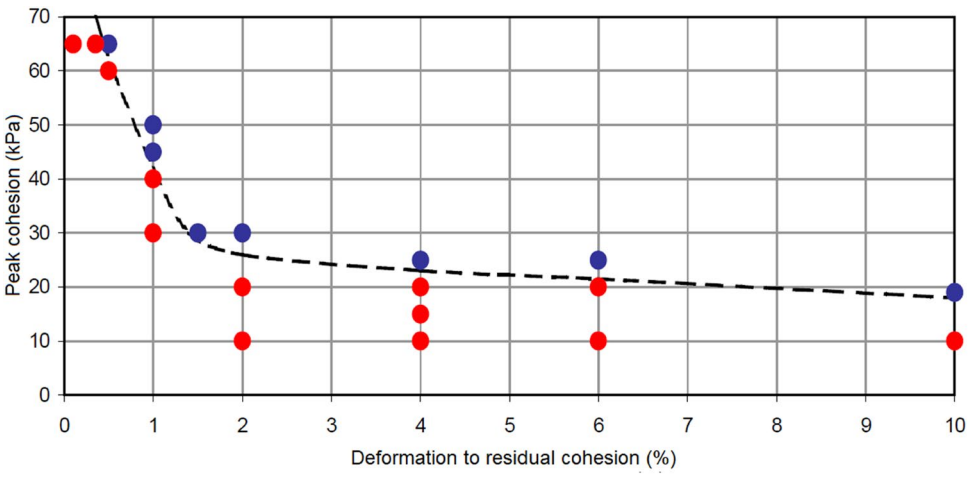

Fig. 15 Consistency between peak cohesion and degree of brittleness: red dots indicate failure before April 1998 and blue dots survival

along horizontal planes, they might develop a somewhat shallower, more planar failure surface even for a slightly more ductile cohesion. But the fact that the differences in behaviour observed for differently oriented tests fall within the scatter of the data suggests that this effect is small.

An independent piece of information tends to confirm this conclusion: the displacements recorded by inclinometer I-3 during its 12 months of operation (during 1997). Figure 18 depicts the inclinometer trace, together with two other traces, which are the expected displacements for a case with very brittle cohesion ($c'_p = 65$ kPa, $\varepsilon_c = 0.005$) when the level of water inside the pond increases by 0.95 m: in one case, this event is assumed to be the first that occurs with the addition of the final 2 m of tailings and water, while in the other case, it is the last one. Both the location and size of the displacement discontinuity are reproduced fairly well. However, a smaller and more

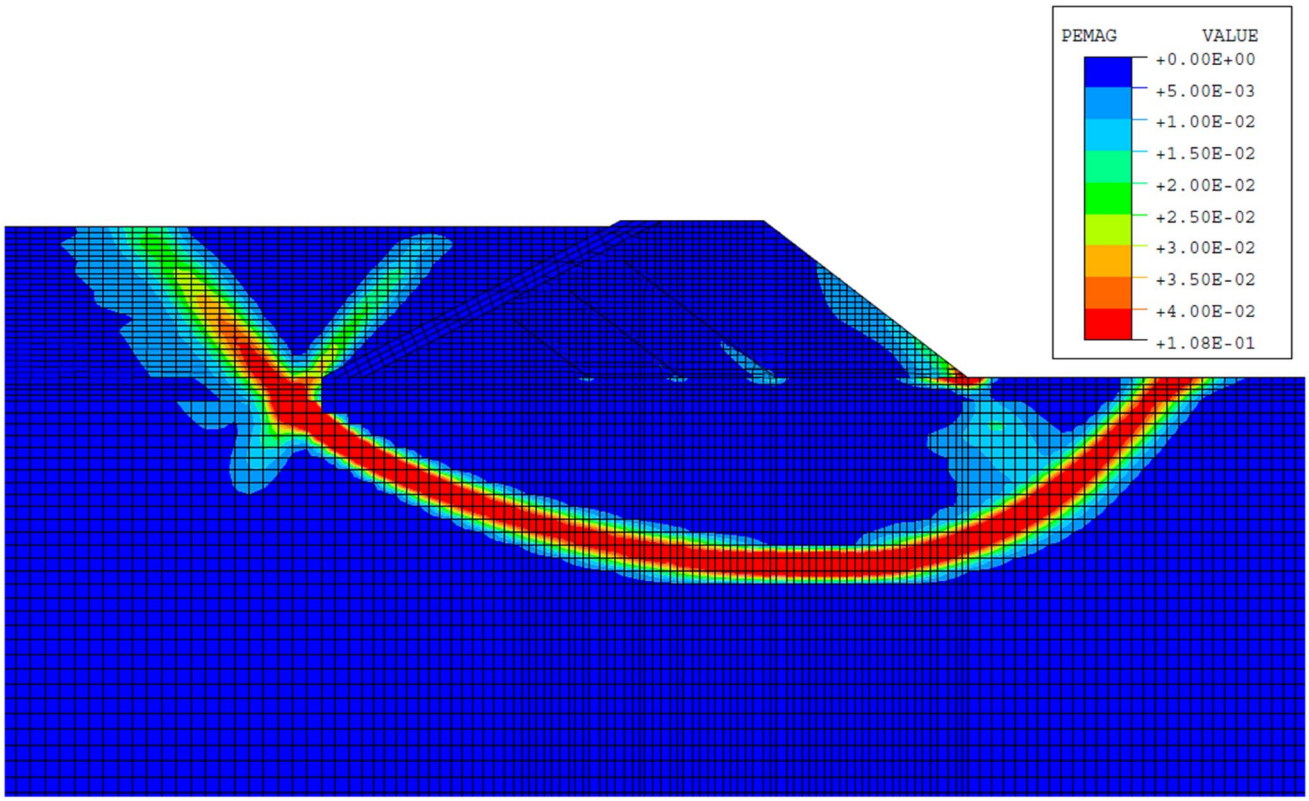

Fig. 16 Plastic strains just before 27 m ($C_v = 0.001$ cm^2/s; $c'_p = 20$ kPa $\varepsilon_c = 0.06$; $\varepsilon_\varphi = 0.10$)

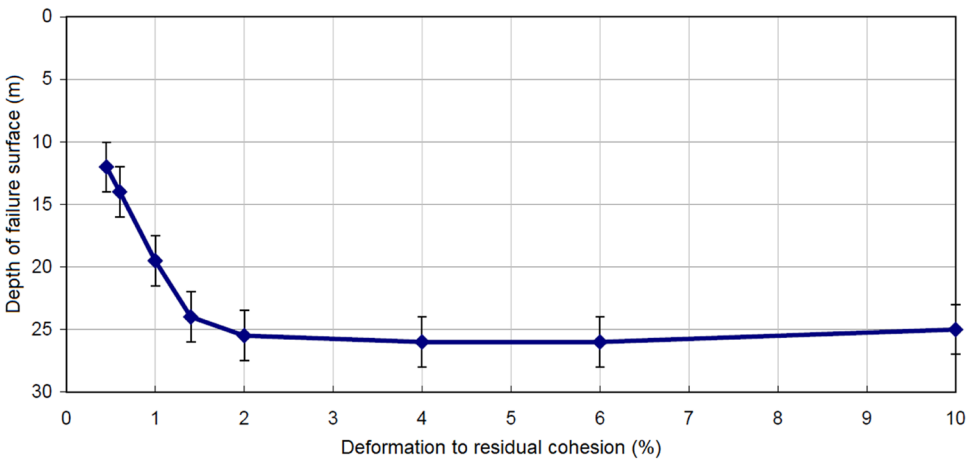

Fig. 17 Depth of the failure surface as a function of the degree of brittleness for failures occurring in April 1998

ductile cohesion (even if able to match the timing of the failure) does not yield the discontinuity at the correct depth.

Other Observations

Several investigations have been conducted to evaluate the influence of other parameters and will be briefly mentioned here. The stiffness of the schists plays a very moderate role in the problem. Failure was studied using two different values of the Young's modulus of the schists: 200 MPa (maintained in most of the analyses) and 100 MPa. The results were very similar in both cases.

The main effect of increasing the friction angle of the tailings was increasing the ratio of the horizontal to the vertical stresses developed. Hence, for a given height of tailings, the loading on the dam is somewhat greater. The tailings were described as an elastoplastic hyperbolic material, with

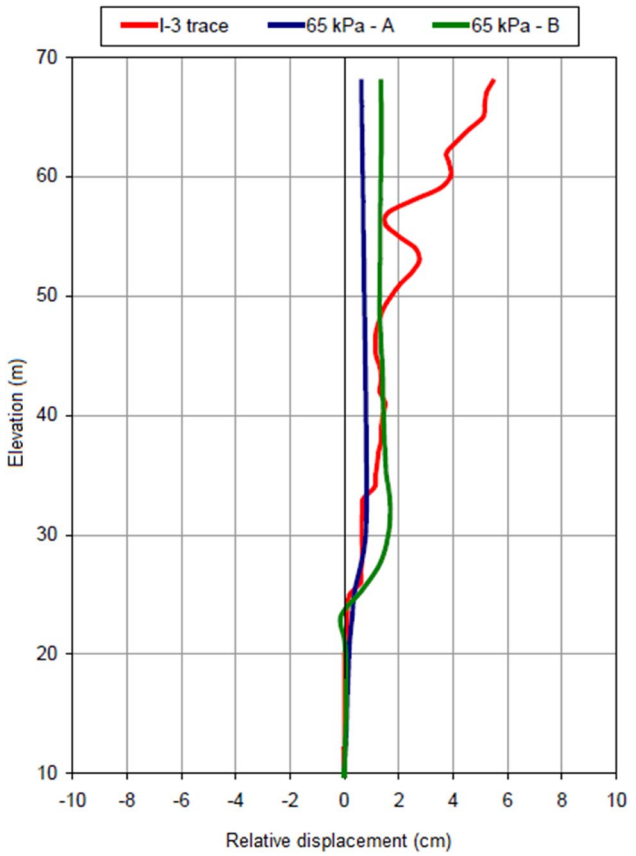

Fig. 18 Trace of inclinometer I-3 compared to those calculated with local tailings elevations of 24 m (**a**) and 26 m (**b**)

high compressibility (Young's modulus $E = 2.6$ MPa) and a strength asymptote derived from a 37° friction angle. As a result, failure occurs slightly earlier because of the increased horizontal forces, but the differences are not large and the failure mechanism is similar; the main observable difference is that the tailings no longer develop shear bands from the upstream toe, but create a plastified region extending over the lower two thirds of their height.

The influence of the small dilatancy (10°) assigned to the alluvium was tested by removing this dilatancy. This change had very little effect on the predictions.

We also studied the effect of delaying the development of the peak stress in the clays. Instead of assuming linear behaviour up to the peak, the stresses were assumed to grow linearly only to 2/3 of the strength; the material then hardened to reach the full strength at 0.05 plastic strains and a brittle response followed as before. Hardening caused plastic deformations to spread over a wide region but, past the peak strength, strain localisation still occurred.

Finally, the effect of the pre-existing level of horizontal stresses in the clays was also investigated. Figure 19 shows the plastic strains at failure with horizontal stresses equal to 0.9 times the vertical stresses ($K_0 = 0.9$). The clays are characterized by $c'_p = 45$ kPa and $\varepsilon_c = 0.01$, a case in which the 27 m dam barely survives with $K_0 = 1$; starting with the deviatoric stresses associated with $K_0 = 0.90$, the dam fails at 25 m, activating a shallow failure surface that agrees well with the observations. For consistency with the timing of the failure, a value of $K_0 = 0.9$ would be possible with a slightly more ductile behaviour than otherwise derived.

The structure of bedding planes within the clays was not introduced in the simulations. Despite that, the geometry of the failure surface (planar, some 10–12 m within the clays) is well reproduced by models with the proper degree of strain softening, but not without it, even with the same average strength along the failure surface; this observation also applies to the horizontal displacements recorded by inclinometer I-3 within the clays. It is therefore clear that brittleness plays the major role for producing the failure characteristics observed in the accident. The structure of the clays may also play a role, though it is probably less important; this role is suggested by the fact that the orientation and dip of the planar failure surface coincide with those of the bedding planes.

The laboratory tests indicated that the clays did not show a greatly decreased strength along subhorizontal planes and that planes located about l0-12 m within the clays were not weaker than at other depths. ln fact, there was no need for either of these things to happen because, if brittleness was properly incorporated, the failure surface already had a natural tendency to occur where and as it did. This view will be reinforced in the next section.

Simulation of Post-liquefaction Events

When liquefaction occurs, shear stresses in the tailings vanish or become very small, and the tailings no longer contribute to the stability of the dam. Instead, they behave as a dense fluid and the forces on the dam increase as a result. When the dam moves and the clays open behind it, the liquefied tailings occupy this space; as they fill the trench progressively opening behind the moving dam, their level decreases and, with it, the forces they apply. This aspect is disregarded in the calculations, as they only span the initial seconds. Indeed, our objective was only to determine the additional changes produced in the geometry of the failure during the initial post-liquefaction events.

Under the new forces arising from liquefaction, inertia forces are no longer negligible. On the other hand, the process is fast compared with excess pore pressure dissipation, and there is no need for coupled calculations. Hence, the solution procedure migrated from implicit to explicit integration. The new calculations start from failure, as encountered in the previous section. The steps were:

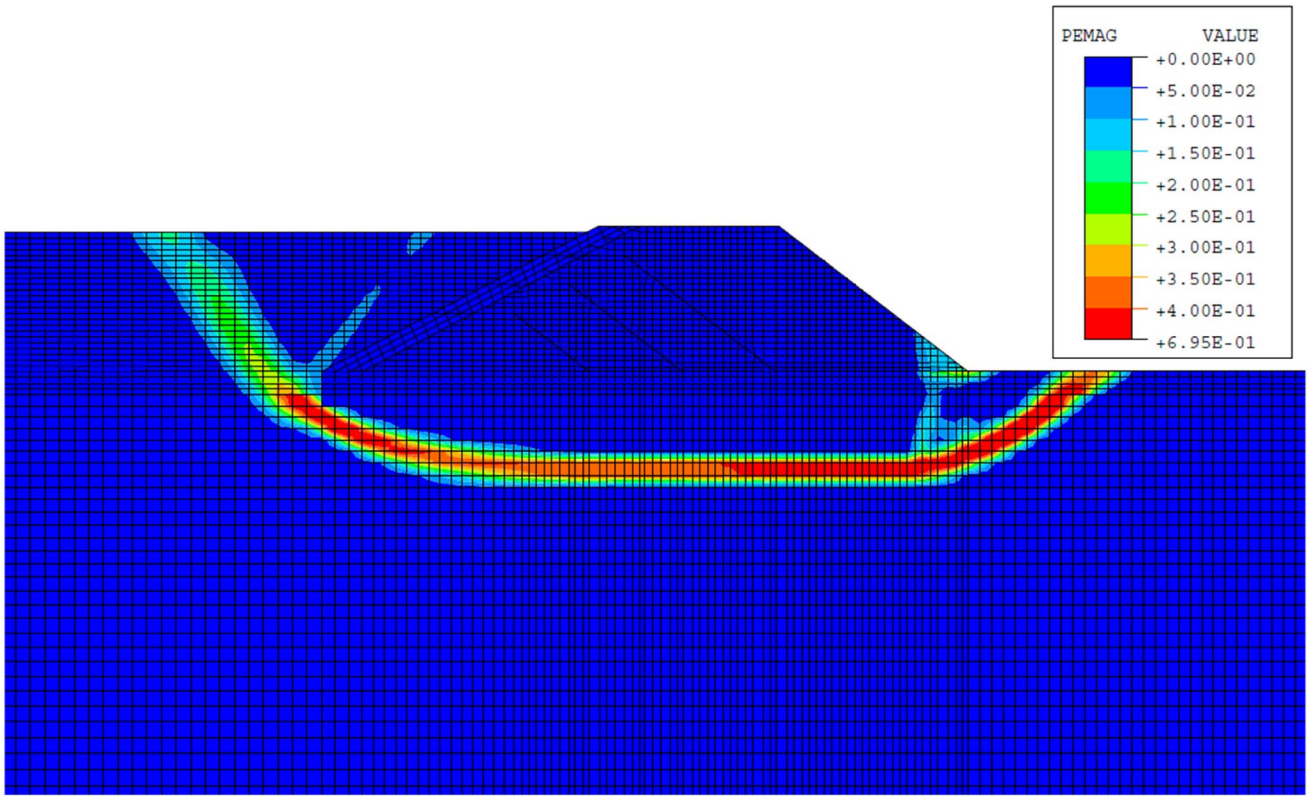

Fig. 19 Plastic strains at 25 m $K_0 = 0.9$

(a) Remove tailings and upstream alluvial, replacing them with the forces they were exerting.
(b) Combine effective stresses and pore pressures in all other materials to provide initial conditions in a total stress formulation.
(c) Adapt the boundary conditions to the total stress formulation.
(d) Adapt the constitutive behaviour to the total stress formulation, with the local strength of the clays depending on the pre-existing effective stresses and deterioration from prior straining.

The above operations are neutral; the dam remains in the same situation of incipient failure. Then, the horizontal forces exerted on the *rañas* and the cement bentonite wall increase towards the post-liquefaction levels. The rate at which the liquefaction process develops is not known with certainty; here, the evolution will be assumed to be linear, over a period of 3 s.

Undrained properties must be used to characterize the elastic part of the response of the clays. The parameters adopted must represent the joint response of the solid skeleton and the water, since the latter will not have time to drain away. Hence, a Young 's modulus of 120 MPa, taken from Eptisa (1998), was used; for the Poisson's ratio, a value of 0.48 seemed reasonable for those conditions.

The migration to the new calculations was performed using 360 material models for the clays. They differ in initial peak strength, residual strength, and the plastic strain over which the transition to the residual strength takes place. They correspond to 30 ranges of effective pressures multiplied by 12 ranges of strain softening. Thus, the post-liquefaction behaviour of the clays was locally consistent with their effective pressures and plastic strains when the tailings liquefied.

For each of the pre-liquefaction calculations conducted, the tailings were assumed to liquefy providing failure was expected at or around a dam height of 27 m. Then, with the new forces generated by the liquefaction, the evolution of the dam was calculated for the first 5 s. Figure 20 is a typical example of the results obtained. It shows the plastic strains and the displaced dam after 5 s for a case when the coefficient of consolidation was 0.001 cm^2/s; cohesion disappeared with strains of 0.005 and friction became residual over 0.1 strains. By then, the dam has already moved some 7 m and a passive wedge of materials was building up ahead of the dam. Behind it, a cavity was growing, which would take advantage of any pre-existing subvertical N-S fissures

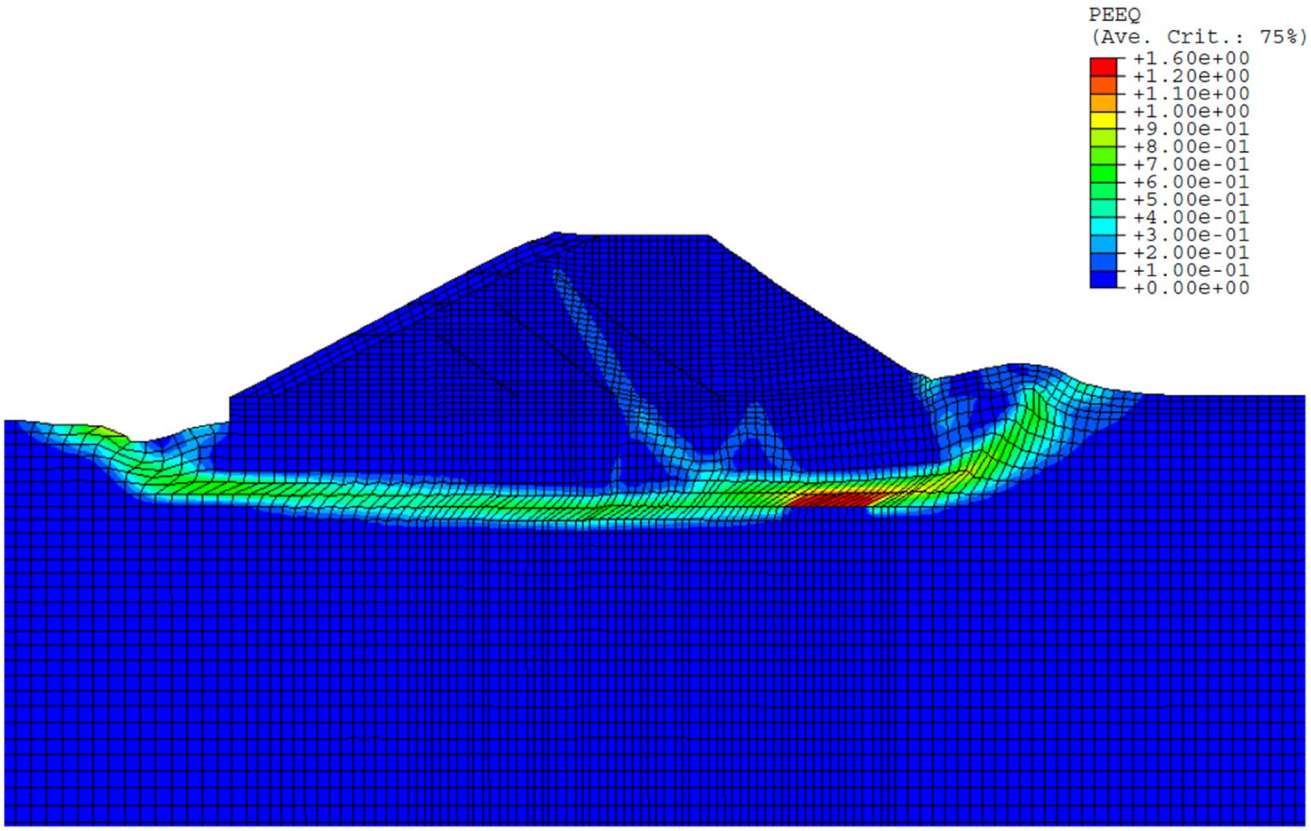

Fig. 20 Displaced dam with plastic strains after 5 s ($C_v = 0.001$ cm^2/s; $\varepsilon_c = 0.005$; $\varepsilon_\varphi = 0.1$)

to localize the incipient trench. The geometry of the failure is clearly consistent with the observations, even though nothing specific has been done to account for the structure of the clays.

Although not shown here, the results are not very different for reasonable variations of the coefficient of consolidation and degree of brittleness. Indeed, the dynamics of the post-liquefaction events do not tend to amplify the differences from the pre-liquefaction phase; rather, they tend to make the results more uniform. The relative insensitivity of the results within the range of variations analysed gives confidence on the geometry of the failure.

The role of progressive deterioration of the clays was also investigated. To this end, the analysis that gave the results presented in Fig. 11 was repeated, but without accounting for any deterioration that might have occurred prior to liquefaction of the tailings. In other words, the clays were still able to develop their peak strength with liquefaction (Fig. 21). As can be seen, the differences are not very large, but the failure surface is now deeper and more smoothly curved: instead of a plane at 10–12 m, it reaches a depth of about 18 m.

This observation clarifies the role of brittleness relative to the failure surface. Brittleness, progressively activated during the construction, was responsible for the shallow, planar character of the failure surface. If the same material had somehow been protected from weakening during construction, the failure surface would have been deeper and more smoothly curved. The failure configuration developed from liquefaction of the tailings is partly inherited from the construction history, due to the brittleness of the clays. It is therefore not surprising that models that do not account explicitly for the brittleness of the clays predict failure surfaces that are deeper and more smoothly curved and hence need to assign a greater role to the clays' structure (Alonso and Gens 2000; EPTISA 1998).

Lessons Learned

The accident experienced at the Aznalcóllar impoundment provides some lessons that may be useful in future occasions. The basic cause of the failure was the homogeneously very low permeability of the 70 m thick clay formation, which was disregarded in the design calculations. The permeability was known, but it is understandable that the designers assumed that Nature would provide some preferential drainage paths in the clays and that a construction lasting 20–25 years would guarantee the dissipation of excess pore

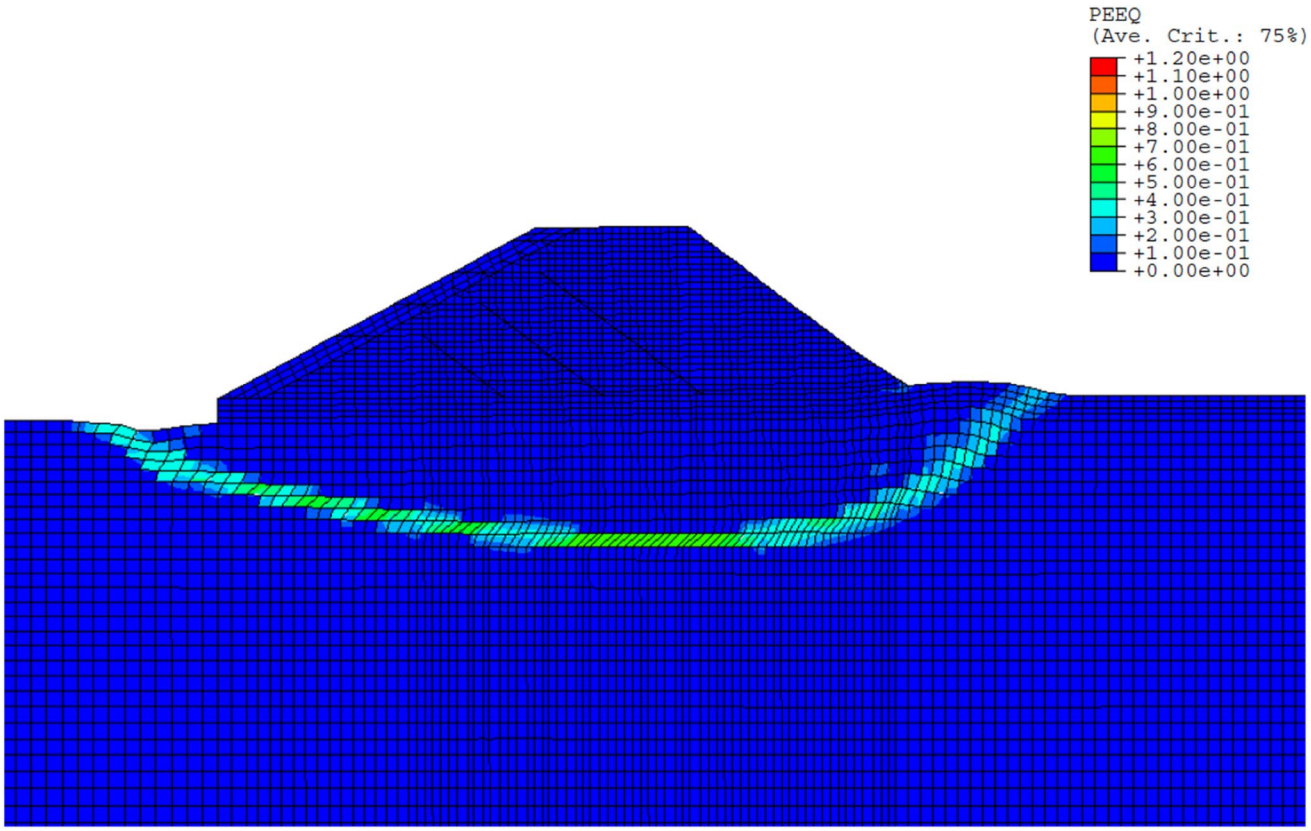

Fig. 21 Displaced dam assuming no deterioration during construction

pressures under the dam. This assumption was in fact wrong and should have been verified. The obvious method would have been to install piezometers that reached into the clays. These would have shown the very slow pace of consolidation and caused a redesign, essentially a wider dam base: since the dam weight did not contribute frictional strength, the only way to improve the sliding stability was to spread the demands over a greater area.

The second key aspect is the brittle behaviour of the clays. When brittleness is suspected (due to pre-consolidation, cementation, etc.), it is important to characterise it. This brittleness would not have been able to manifest itself if things had worked as planned, because the clays would never have exceeded their peak strength, making their post-peak behaviour irrelevant. But disregarding the slow consolidation of the clays provided the conditions for reaching the peak strength and activating the brittle behaviour. The occasion could have been different, e.g. an earthquake much greater than the design event. Whatever the cause, if the post-peak response is brittle, it is worth considering whether perhaps the safety factor should be increased to decrease the chances of reaching the peak, because the consequences of doing so are far worse than with a ductile response.

The next question is whether the previous shortcomings could have been evinced by suitable instrumentation and monitoring. Regarding the slow dissipation of the pore pressures in the clays, the answer is clear: the installation of piezometers monitoring the evolution of pore pressures in the clays would have made the problem obvious. But there are practically no means of detecting the silent progress of an impending brittle failure which, once triggered, inevitably leads to a catastrophe. In this sense, neither deeper nor more numerous inclinometers would have perceived anything because there was nothing to perceive. The only solution to the problem of a brittle post-peak behaviour is to make sure that the post-peak regime is not reached.

Concluding Remarks

The consolidation of the clays under the dam was far from complete when failure occurred; also, the process of failure initiation and development shows that the brittleness of the clays played a major role in the accident, as it allowed a progressive failure with the average strength mobilised at failure substantially below the peak strength. The fact that

those two aspects had not been adequately considered led to a design considerably less safe than intended.

The dam was probably very near collapse already in 1987 when it reached an elevation of 20 m. Progressive failure started during 1986–87, but the large increase in width adopted, while the height grew from 20 to 25 m from 1988 to 1990, allowed marginal stability; had construction proceeded along the lines implemented until 1987, failure would have probably occurred much sooner. From 1991 to 1995, the dam height essentially remained constant; this gave time for some pore pressure dissipation and a small increase in safety, which allowed 2 m to be added to the height until failure finally occurred in April 1998.

The strength and consolidation properties determined by Alonso and Gens (2000) are consistent with the timing of the failure. This consistency would also be maintained if the peak cohesion were lower but compensated by a less brittle behaviour. But their cohesion and degree of brittleness are also consistent with the geometry of the failure developed (planar, some 10–12 m within the clays) in the absence of significant influence from the clays' structure; the same seems to apply to the displacement discontinuity recorded by inclinometer I-3. Both features are lost if cohesion and brittleness are changed substantially, even if the change are consistent with the timing of the failure.

The brittleness of the clays, which was activated during the construction, plays an essential role in the geometry of the failure surface. The same average mobilised strength in a ductile material would result in a curved and deeper failure surface than experienced. A somewhat similar conclusion is reached if the material, though brittle, is assumed to have suffered no weakening prior to failure.

Failure started at the upstream toe, as well as along a curved surface surrounding the downstream toe, and surfaced about 20 m downstream. The central parts of the failure surface, especially its upstream section, were the last to develop. Incipient failure produced liquefaction of the tailings, which significantly increased the forces on the dam. The dynamics of the post-liquefaction situation have been modelled over the first 5 s. The characteristics of this phase are such that pre-existing differences, from varying initial hypotheses, do not tend to grow to vastly different outcomes. The forces exerted by the tailings following liquefaction produced accelerations greater than 1 m/s^2. The ulterior deceleration was probably a consequence of a decreasing level of liquefied tailings behind it. The failure event must have been completed in a fraction of a minute.

The calculated failure surface reproduces what was observed at the site well, even though no provisions were made to account for the structure of the clays. This is consistent with the fact that the clays appear to be a massive formation, with little anisotropy or inhomogeneity and with somewhat elusive subhorizontal inhomogeneities. Although a subhorizontal structure would obviously help to localize the failure, the analyses indicate that the latter would have taken place in approximately the same location, even in the absence of any structure.

The same applies to the subvertical fissures limiting the west and north side of the slide. The western boundary of the slide is a consequence of the fact that the failure surfaces go through the upstream toe of the dam. The location of the NE-SW tear at the north end of the slide, which started at the northeast end of the pyrite pond, was forced by the liquefaction of the tailings, which caused a large increase in forces on the dam, but only south of this point. Hence, that point marked the origin of a tear that propagated towards the NE; if a subvertical NE–SW fissure existed, it would obviously have helped to localize the tear, but it would have occurred there in any case.

The progressive failure made possible by the brittleness of the clays would have been difficult to anticipate with the instruments installed. The strength deterioration progressed gradually, possibly with few symptoms, as construction proceeded; the failure event was then sudden. Past the initial failure, the strength along the failure surface was decreased; furthermore, once the tailings behind the dam liquefied, the horizontal forces exerted increased, and a large failure was unavoidable.

References

Alonso EE, Gens A (2000) Failure of the mine tailings pond of Aznalcóllar. Court's Experts Report, 30 March [in Spanish]

Alonso EE, Gens A (2006a) Aznalcóllar dam failure. Part 1: field observations and material properties. Géotechnique 56(3):165–183

Alonso EE, Gens A (2006b) Aznalcóllar dam failure. Part 3: dynamics of the motion. Géotechnique 56(3):203–210

Alonso EE, Zabala F (2012) Failure mechanisms in brittle soils: a dam failure revisited with the material point method. In: Khalili, N, Oeser M (eds) Computer methods for geomechanics: frontiers and new applications. Proc, international conf of international assoc for computer methods and advances in geomechanics, Melbourne, vol 1, pp 377–38

Alonso E, Pinyol NM, Puzrin AM (2010) Geomechanics of failures. Advanced topics, Chapters 4 and 6. Springer, Dordrecht

Botín JA, Ramírez-Oyanguren P (1999) Failure mechanisms of the tailings pond of the Aznalcóllar mine. Industria y Minería 355:25–32 **[in Spanish]**

Cooper S, Rodríguez MD, Galera JM, Pozo V (2019) Stability considerations for slopes excavated in fine hard soils/soft rocks at Cobre Las Cruces mine, Sevilla, Spain. J S Afr Inst Min Metall 119:647–659

EPTISA (1998) Investigation of the failure of the Aznalcóllar tailings dam. Minas de Aznalcóllar (Seville), Report, October

Fernández Blanco S (1979) Study of the geotechnical properties of the Guadalquivir blue clays with special application to long-term stability of natural slopes. PhD Thesis, School of Civil Eng, Madrid, June [in Spanish]

Fernández Rubio R (ed) (1999) Proc, IMWA Congress, Sevilla, Spain. https://www.imwa.info/imwaconferencesandcongresses/proceedings/182-proceedings-1999.html

Galera JM, Checa M, Pérez C, Williams B, Pozo V (2009) Detailed characterization of the Guadalquivir blue marls by in-situ and laboratory testing. Ingeopress 186:16–22 **[in Spanish]**

Gens A, Alonso EE (2006) Aznalcóllar dam failure. Part 2: stability conditions and failure mechanism. Géotechnique 56(3):185–201

Geocisa (1996a) Report on stability. Tailings pond of the Aznalcóllar mine. Report 184, March [in Spanish]

Geocisa (1996b) Enlargement of the tailings pond dam at the Aznalcóllar mine. Report, June [in Spanish]

Geocisa (1998) Status Report for 1997. Instrumentation of the tailings pond dams. Aznalcóllar mine. Report SE-456, March [in Spanish]

Geocisa (2000) Analysis of factors possibly involved in the failure of the dam of the tailings pond at Aznalcóllar (Sevilla). Report [in Spanish]

Gibson RE (1958) The progress of consolidation in a clay layer increasing in thickness with time. Géotechnique 8(4):171–182

HKS (Hibbitt, Karlsson, & Sorensen) (1998a) ABAQUS/standard users' manual, Vers. 5.8, Pawtucket, Rhode Island

HKS (1998b) ABAQUS/explicit users' manual. Vers. 5.8, Pawtucket, Rhode Island

Intecsa (1978) Final project for the tailings pond. Vol I to V, November [in Spanish]

McDermott RK, Sibley JM (2000) The Aznalcóllar tailings dam accident—a case study. Min Resour Eng 9(1):101–118

Olalla C, Cuéllar V (2001) Failure mechanism of the Aznalcóllar dam, Seville, Spain. Géotechnique 51(5):399–406

Oteo C, Sola P (1993) Stability problems in slopes constructed on Spanish 'blue marls'. In: Anagnostopoulos A, Frank R, Kalteziotis N, Schlosser F (eds) Geotechnical engineering of hard soils—soft rocks. Balkema, Rotterdam, pp 1147–1154

SIMULIA (2019) Abaqus analysis user's guide. Vers. 2020

Skempton AW (1964) Long-term stability of clay slopes. Géotechnique 14:77–101

Zabala F, Alonso EE (2011) Progressive failure of Aznalcóllar dam using the material point method. Géotechnique 61(9):795–808